Polymer Chemistry

ROYAL SOCIETY OF CHEMISTRY

PAPER

View Article Online
View Journal | View Issue

Cite this: *Polym. Chem.*, 2021, **12**, 216

Direct synthesis of light-emitting triblock copolymers from RAFT polymerization†

Anielen H. Ribeiro,[a] Joris Haven,[b] Axel-Laurenz Buckinx,[b] Michelle Beuchel,[a] Kai Philipps,[a] Tanja Junkers *[b] and Jasper J. Michels *[a]

We introduce a straightforward and clean method to synthesize pi-conjugated triblockcopolymers (tri-BCPs) using RAFT polymerization. The strategy circumvents known disadvantages associated with transition metal- or nitroxide-mediated radical polymerizations. The method involves the synthesis of a conjugated macroinitiator, in this case based on poly(dioctylfluorene) (PFO), followed by a RAFT polymerization of styrene or methyl acrylate. The difference in chemistry and polarity between these monomers confirms the versatility of the method. As shown by NMR and GPC, the molecular weight of the obtained polystyrene-(PS-*b*-PFO-*b*-PS) and poly(methyl acrylate)-(PMA-*b*-PFO-*b*-PMA) tri-BCPs is well-controlled and exhibits a relatively low dispersity of $Đ < 2$. Thermally annealed films of the nonpolar PS-*b*-PFO-*b*-PS exhibit domains containing nanostructures with a lateral periodicity commensurate with classical BCP phase separated morphologies. PMA-*b*-PFO-*b*-PMA self-assembles in water, whereby the PFO blocks partly organize into the β-phase. The marked red-shift of the luminescence spectrum confirms complete energy transfer from the amorphous to the β-phase fraction, which can be fully barred by dissolving the nano-assemblies through titration of THF into the aqueous dispersion.

Received 21st September 2020,
Accepted 17th November 2020

DOI: 10.1039/d0py01358g

rsc.li/polymers

Introduction

Semiconducting block-copolymers (BCPs) have attracted considerable attention for optical, optoelectronic and biomedical applications.[1–5] The reason for this is that BCPs combine two (or more) functionalities within a single polymer. Semiconducting BCPs may be all-conjugated, *i.e.* combining different (opto)electronic functionalities,[6] or partly conjugated, combining semiconducting or light-emitting functionality with a non-conjugated block.[7,8] As for the latter, the typically more flexible non-conjugated block provides solubility, dispersability[9,10] and/or mechanical properties.[11,12] BCPs are known for their capability to self-assemble or microphase separate into thermodynamically relaxed nanostructures, which can be tailored to suit various applications.[5,13–15] The extent and dynamics of phase separation depend on block length and polarity, chain flexibility, glass transition temperature, *etc*.[16] If the contour length of the conjugated block is small relative to its persistence length, rod-coil BCPs are obtained for which additional contributions, such pi-stacking interactions, may give rise to non-classical morphologies, extending the portfolio of functional nanostructures.[17–20]

The synthesis of conjugated BCPs may either proceed *via* prior polymerization of the separate blocks and subsequent ligation *via* click chemistries, or *via* chain extension of the first block in a subsequent polymerization.[21] Both cases require a conjugated polymer that is end-functionalized with an appropriate reactive unit, either to provide a point for coupling/clicking, or as macroinitiator. End-functionalities are introduced through the use of functional end-capping agents in classical transition-metal catalyzed cross coupling reactions,[20] or by initiating chain growth from a dual-initiator moiety, *i.e.* in case of poly(*p*-phenylenevinylene) (PPV)-type conducting blocks.[22,23] In the chain ligation method,[24] the coupling of the preformed blocks has, for instance, been accomplished by creating an ester linkage,[25,26] quenching an anionic living coil polymer[27–29] or click reaction.[30] In addition, Yamamoto coupling[31] and click chemistry[32] have been used to prepare all-semiconducting BCPs. A general drawback of grafting-to approaches is that they suffer from steric effects arising from the reaction between two bulky precursors.[33] During the chain-extension approach, which does not bear this disadvantage and requires a reduced number of reaction steps, the first block functions as a macroinitiator for the formation of the second.[34] In case of conjugated-nonconjugated BCPs, which form the focus of this work, the flexible block is often grown *via* atom transfer radical polymerization (ATRP),[7,8,35–40]

[a]*Max Planck Institute for Polymer Research, Ackermannweg 10, 55128 Mainz, Germany. E-mail: michels@mpip-mainz.mpg.de*
[b]*Polymer Reaction Design Group, School of Chemistry, Monash University, 19 Rainforest Walk, Clayton, VIC 3800, Australia. http://www.polymatter.net*
†Electronic supplementary information (ESI) available. See DOI: 10.1039/d0py01358g

although nitroxide-mediated radical polymerization (NMP),[41–43] anionic living polymerization[44,45] and ring-opening metathesis polymerization (ROMP)[46–48] have also been used. For completeness, we note that all-conjugated BCPs have been obtained using the grafting-from method in combination with oxidative polycondensation,[49] catalyst transfer condensative polymerization[50] and Suzuki polycondensation.[51–53] Despite their regular use, the above mentioned macroinitiator pathways all have disadvantages, in particular relating to the use of (toxic) transition-metal catalysts (including ATRP and ROMP), and/or a high reaction temperature (NMP). The latter imposes the risk of side reactions of the conjugated polymer and largely excludes the use of methacrylates[54] for the nonconjugated block. Further, all these methods require the introduction of suitable initiator functionalities, which typically are not compatible with the conditions of the conjugated polymer synthesis. Their introduction is thus often tedious.

In this work, we circumvent these disadvantages by synthesizing fluorescent conjugated-nonconjugated BCPs by means of reversible addition fragmentation chain transfer polymerization (RAFT). The RAFT approach is highly attractive as it is compatible with a broad range of monomers,[55–58] without requiring metal catalysts or high temperature.[59] To our knowledge, a limited number of studies exist on the use of RAFT in combination with conjugated systems, and only concerning relatively short conjugated moieties. Xiao *et al.*[60] have applied RAFT to grow poly(*N*-isopropylacrylamide) chains from a bifunctional terfluorene segment. Chen *et al.*[61] applied RAFT to grow polystyrene or polyacrylate from units based on quaterthiophene, oligothiophene or perylene diimide. The method has so far not been used for the fabrication of true block-copolymeric functional materials.

We here show that RAFT polymerization can be effectively and quite generally applied for this purpose, by demonstrating the synthesis of two semiconducting triblockcopolymers (tri-BCPs) based on poly(9,9-dioctyl-9*H*-fluorene-2,7-diyl) (PFO), combined with either polystyrene (PS) or poly(methyl acrylate) (PMA) presenting, respectively, a hydrophobic and a hydrophilic flexible block. We use a simple, yet efficient approach to introduce the RAFT-typical endgroup on the conjugated polymer, which can be translated later also to other polymers.

PFO, arguably the best-known blue emitting conjugated polymer, combines thermal and chemical stability with high fluorescence quantum yields and solubility in a range of apolar solvents.[7,15,62] Besides an amorphous and (liquid) crystalline phases,[63,64] PFO is known to form a metastable β-phase, comprising planar chain segments in which the monomers adopt an all-gauge conformation. This results in an extended conjugation length, leading to a red-shift in of the absorption and fluorescence spectrum and increased luminescence quantum yield.[65] In what follows, we show that a key step in our novel procedure is the conversion of distyryl end-capped PFO into a RAFT macroinitiator, while avoiding preliminary polymerization of the functionalized PFO itself. A linear increase in molecular weight with conversion during subsequent RAFT polymerization of the co-monomer, as well as a low dispersity of the resulting BCP, demonstrate that the polymerization is well-controlled. Although this work puts emphasis on the synthetic procedures, we augment our study with preliminary data on the self-assembly of the PS-PFO-PS and PMA-PFO-PMA tri-BCPs, respectively in thin film and aqueous dispersion.

Results and discussion

RAFT is a representative of reversible deactivation radical polymerization (RDRP), based on a degenerative transfer equilibrium between active and dormant chains.

We commenced with the synthesis of a di-end-functional PFO homopolymer precursor, to be converted into the macroinitiator by subsequent functionalization with a RAFT agent in a 1,2 radical insertion reaction. Distryryl-capped PFO **2** was obtained using the Yamamoto cross coupling reaction[66,67] in the presence of 4-bromostyrene (Scheme 1). Although the Yamamoto method has been known for quite some time, we chose this approach for its practical convenience. Only a single (in our case commercially available) monomeric precursor is required, which guarantees reaching a decent molecular weight without having to (i) either delicately balance an A–A : B–B co-monomer ratio due to the Carothers prerequisite, or (ii) embark on a more involved precursor synthesis of an A–B monomer, *i.e.* prerequisites that would apply to, for instance, a Suzuki polycondensation. Irrespective of the fact that some studies seem to advocate the Yamamoto route over, for instance, the Suzuki polycondensation to fabricate polyfluorenes,[68,69] we stress that our approach is general. As long as both ends of the conjugated polymer are styryl- or vinyl-capped, any transition metal-catalyzed cross coupling polymerization can in principle be used to fabricate the semiconducting precursor block.

We took the capping agent-to-monomer ratio such to limit the molecular weight of the functionalized PFO at $\check{M}_n$ = 17 000 g mol^{-1} (see Experimental section). Furthermore, since our approach to synthesizing the PFO block has not been specifically optimized to control chain length, we applied a

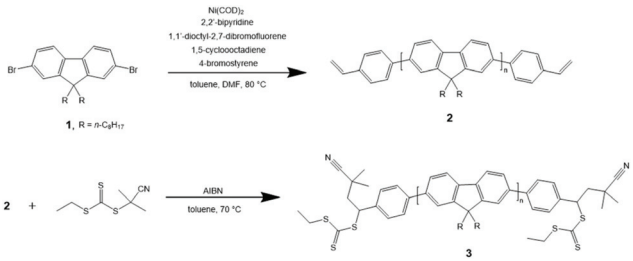

Scheme 1 Synthesis of RAFT macroinitiator di-CPETTC-PFO **3** *via* (i) Yamamoto polymerization of dibromodioctylfluorene **1** to distyrene end-capped PFO **2** and subsequent functionalization with 2-cyano-2-propyl ethyl trithiocarbonate (CPE-TTC); COD = cyclooctadiene; AIBN = 2,2′-azobis(2-methylpropionitrile).

long extraction procedure (see Experimental section) not only to remove impurities, but also to wash out the low molecular weight fraction in order to limit molecular weight dispersity. The ^{1}H NMR spectra of the distyrene-PFO homopolymer (ESI, Fig. S1†) shows signals at 5.31 ppm, 5.84 ppm and 6.80 ppm, attributed to the vinyl end groups.

The styryl endgroup is ideal to introduce a further functionality *via* a 1,2-radical insertion reaction. Its reactivity is comparable to styrene, which is a common monomer to be polymerized *via* RDRP. The PFO thus serves as a kind of macromonomer. Yet, due to its specific reactivity, when reacted with a RAFT agent, it will undergo a single insertion reaction rather than polymerization. It is typical for a RAFT process to commence with a 1,2 insertion reaction (conversion from pre- to main equilibrium), hence side reactions would be scarce. Polymerization of the PFO macromonomer is further sterically and entropically disfavored.

Hence, in the following step distyryl-capped PFO **2** was functionalized with the RAFT agent 2-cyano-2-propyl ethyl trithiocarbonate (CPETTC) in the presence of azobis(isobutyronitrile) (AIBN), resulting in the bifunctional macroinitiator di-CPETTC-PFO **3**. We used a relatively large excess of RAFT agent, while maintaining a low concentration of AIBN to drive the reaction to completion, and to stay on the side of caution with regards to an undesired termination reaction with AIBN-derived cyanoisopropyl radicals. AIBN was replenished intermittently as the reaction proceeded. No insoluble material was obtained, nor was a significant increase in the molecular weight observed, indicating that our strategy was successful. The synthesis of our macroinitiator di-CPETTC-PFO **3** was confirmed by the complete disappearance of the vinyl signals (5.31, 5.84 and 6.80 ppm) in the ^{1}H NMR spectrum (see ESI, Fig. S2†), together with the appearance of the new signals at 5.53, 3.37, 2.4 and 1.58 ppm, ascribed to the CPETTC moiety. It should be noted that the PFO **2** features styryl endgroups on either side of the chain. Hence, RAFT endgroups will be added to both sides and chain extension will lead to symmetric triblock copolymer structures.

In the final step we performed the actual chain extension of the non-conjugated blocks from di-CPETTC-PFO macroinitiator **3** *via* RAFT polymerization. To show the generality of the method, we used styrene, as well as the more polar methyl acrylate to give the corresponding PS-*b*-PFO-*b*-PS and PMA-*b*-PFO-*b*-PMA tri-BCPs **4** and **5**, respectively, in a controlled fashion (see Scheme 2). In case of the synthesis of **4**, the initiator 1,1′-azobis(cyanocyclohexane) gave somewhat higher conversions than observed when using AIBN. As shown below, tri-BCP **5** is amphiphilic owing to the strong difference in polarity between the PFO and the poly(methyl acrylate) blocks. Indeed, this material undergoes self-assembly in aqueous solution. However, prior to expanding on the self-assembly properties of both tri-BCPs, we demonstrate more quantitatively the effectiveness of our procedure by providing a detailed kinetic analysis of the RAFT polymerization towards **4**.

During the reaction, samples were taken at five time intervals and subsequently analyzed by means of ^{1}H NMR and GPC

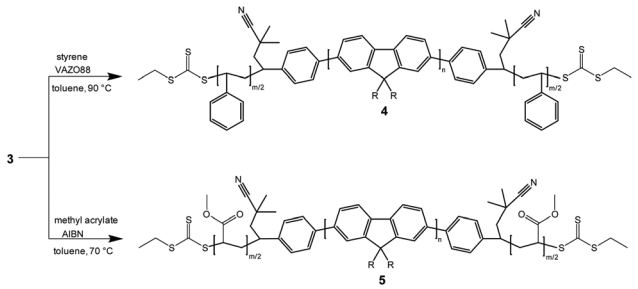

Scheme 2 Synthesis of triblockcopolymers poly(styrene)-*b*-poly(dioctylfluorene)-*b*-poly(styrene) **4** and poly(methyl acrylate)-*b*-poly(dioctylfluorene)-*b*-poly(methyl acrylate) **5** *via* RAFT polymerization starting from macroinitiator di-CPETTC-PFO 3; VAZO-88 = 1,1′-azobis (cyanocyclohexane).

to monitor chain growth. The ^{1}H NMR spectra of the five samples are shown in Fig. S3 of the ESI.† At t = 0 minutes, the spectrum only shows signals corresponding to the PFO homopolymer. As the reaction proceeds, polystyrene chain growth is indicated by the appearance and growth of respective signals. To provide proof that the PFO block and the growing polystyrene chain are indeed covalently attached, we performed DOSY analysis (see Fig. 1a).[70] Besides a chloroform signal, the spectrum clearly shows one single diffusing polymeric species containing both PFO- and polystyrene residues, as indicating by the color-shaded regions of the ^{1}H NMR spectrum. The corresponding diffusion coefficient of ~10^{-6} cm^2 s^{-1} is a typical value for polymer diffusivity in dilute and semidilute solution.[71]

By quantitative comparison of the integral values of the ^{1}H NMR signals of PFO, having aliphatic residues represented at 0.85 ppm and 1.20 ppm, with the those of the signals at 1.49 ppm and 1.90 ppm marking the growing polystyrene blocks (see ESI, Fig. S3†), we estimated the number-average molecular weight ($\bar{M}_n$) of the resulting tri-BCP. Concurrently, GPC shows that the unimodal molecular weight distribution shifts to higher molecular weights with progressing polymerization (see Fig. 1b) without exhibiting significant broadening.

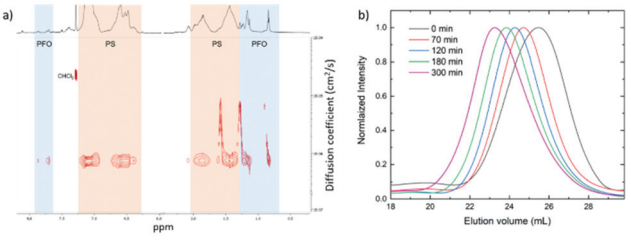

Fig. 1 (a) DOSY ^{1}H NMR spectrum of PS-*b*-PFO-*b*-PS tri-BCP **4** in deuterated chloroform. The shaded blue and orange regions represent signals corresponding to the PFO and polystyrene block, respectively. (b) GPC elutograms of samples of PS-*b*-PFO-*b*-PS tri-BCP **4**, taken at different time intervals during the RAFT polymerization of styrene from macroinitiator di-CPETTC-PFO **3**. The GPC runs were performed against polystyrene standards, using THF as the mobile phase.

This again proves the absence of homopolymerization and shows that the growing polystyrene chains are initiated from the PFO blocks. Plotting $\bar{M}_n$ obtained from NMR and GPC as a function of styrene conversion (Fig. 2, black and red symbols) reveals a linear behavior, as is expected for well controlled RAFT polymerization. Further, no significant increase in dispersity is observed, indicating a comparatively good control ($Đ$, blue symbols).

The fact that molecular weight of distyryl PFO precursor **2**, determined *via* end group analysis in NMR agrees well with the number obtained by GPC (*i.e.* left-most black and red points in Fig. 2), strongly supports the notion that the PF has indeed been styryl-capped at both chain ends. In other words, the pre-assumption of double capping in NMR has, in effect, been confirmed by GPC.

We note that the agreement between the estimates obtained from NMR and GPC is quite good, despite the fact that both data may be subject to some uncertainty. In case of NMR line broadening may affect the numbers somewhat, whereas for GPC the considerable chain stiffness of the PFO block[72] might lead to some over estimation of the molecular weight at low styrene conversion. The slight deviation from linearity in the GPC data might be due to a non-trivial change in the tri-BCP's hydrodynamic volume upon the extension of the polystyrene block. Such deviant behavior may be associated with (i) the considerable difference in chain stiffness between PFO and polystyrene, which includes the calibration standards,[73–75] and/or (ii) a difference in compatibility between the blocks with the stationary and/or the mobile phase during GPC.[76] Yet, the observed deviation in GPC is not very large. Besides NMR and GPC, we have attempted to characterize macro-RAFT-initiator **3** using mass spectrometry in combination with electrospray ionization (ESI-MS). Unfortunately, no polymer spectrum was detectable, likely due to the fact that already for the PFO block alone the molecular weight significantly exceeds values considered ideal for this method.[77]

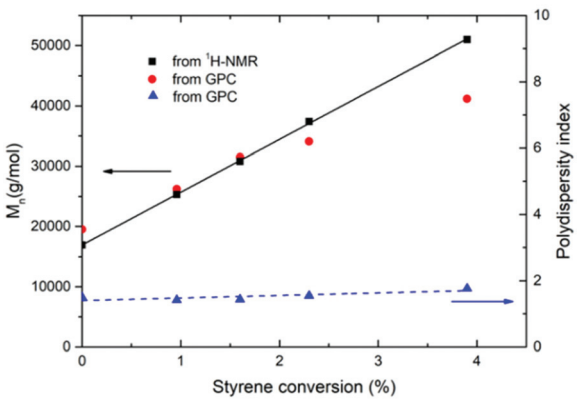

Fig. 2 Number-average molecular weight ($\bar{M}_n$) and polydispersity index ($Đ$) of PS-*b*-PFO-*b*-PS tri-BCP **5**, plotted as a function of styrene conversion during RAFT polymerization. The plot represents data obtained from ^{1}H NMR and GPC, as outlined in the legend. The solid and dashed lines represent empirical linear fit of the data.

In a first conclusion, it can be safely summarized that the RAFT polymerization proceeds well, and in line with expectations. The presence of the PFO does not interfere with the RDRP process, and generally, high quality block copolymers are obtained. This opens the door to block copolymers containing any RAFT-compatible monomer, which can span from styrene over vinyl acetate to water-soluble acrylamides.

The use of conjugated-nonconjugated BCPs as an active layer in optoelectronic devices requires control of self-assembly during solution film-processing and/or post-treatment. Depending on the application, microphase separation, as well as sub-molecular organization within the different domains, is desired or to be suppressed. For this reason, we proceed with a brief discussion of the morphological behavior of thin films of tri-BCP **4**, when subjected to thermal annealing. Since PFO is known to already exhibit a plurality of phases by itself,[78,79] it is of particular interest to reveal any effect on structure formation associated with the presence of two different blocks. For this reason, we compare the behavior of films of **4** with that of distyryl-PFO **2** as a reference. The films (90 nm), prepared by spin-coating onto glass substrates, were heated at 250 °C for 2h, *i.e.* significantly above the glass transition temperature (T_g) of both PFO and polystyrene[80,81] and subsequently conditioned at 130 °C for 17 h.

The AFM phase images recorded on the polymer films (Fig. 3) reveal a clear difference between the PS-*b*-PFO-*b*-PS tri-BCP **4** and the distyryl-PFO reference. Although both samples suffer from minor measurements or casting artefacts (clearly discernible black defects or spots), it is easily seen that whereas the film of distyryl-PFO is relatively featureless, the one of the tri-BCP reveals the formation of "macrodomains" with typical sizes in the range 100–1000 nm. Within these domains a micromorphology can be discerned comprising a disordered lamellar structure with a typical feature size of ~25 nm. Although tri-BCP **4** behaves clearly different in comparison to the PFO reference, the observed structure certainly deviates from a highly ordered classical BCP microphase separated morphology.[82]

Nevertheless, the typical size of the small lamellar features is in principle consistent with BCP micro-phase separation. Verduzco *et al.*[83] observed a somewhat similar structure in solvent vapor-annealed films of the all-conjugated BCP poly-

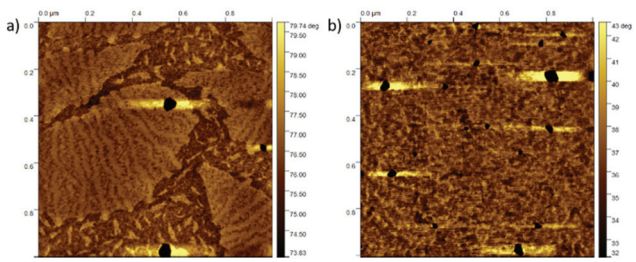

Fig. 3 (a) AFM phase image of a film of PS-*b*-PFO-*b*-PS tri-BCP **4**, spin-coated from chloroform and annealed at 250 °C for 2 h and subsequently conditioned at 130 °C for 17h. (b) AFM phase image of a film of distyryl-PFO **2** that received the same treatment.

thiohene-*b*-polyfluorene, but did not report the appearance of macrodomains. Perhaps our non-classical morphology results from interference between BCP microphase separation and crystallization of the PFO block. A full understanding of the phase behavior of tri-BCP **4** would require extensive morphological investigation, which we consider outside of the scope of this work.

In the next step, we extended the scope of our method towards PMA-*b*-PFO-*b*-PMA tri-BCP **5** (see Scheme 2), prepared from di-CPETTC-PFO precursor **3** using the same RAFT conditions as for tri-BCP **4**, though replacing styrene with methyl acrylate. The molecular weight distribution of the final product is shown in Fig. 4. Tri-BCP **5** has a number average molecular weight of $\bar{M}_n$ = 21 120 g mol^{-1} and a dispersity of 1.7 (see Experimental section for details). The reason for the fact that the molecular weight of tri-BCP **5** is not significantly higher than that of the PFO block itself, is that we deliberately kept the length of the PMA chains low. The aim of the synthesis of tri-BCP **5** was, besides demonstrating the generality of our synthetic approach, to test if micelle-like assemblies[84] would form in aqueous environment, whereby the methyl acrylate block serves as a neutral but polar head group. Previous work has shown that the stability of self-assembled structures from amphiphilic BCPs decreases significantly if the size of the hydrophilic/polar block (significantly) exceeds that of the hydrophobic block.[85,86]

We produced micelle-like assemblies of BCP **5** using a flow set-up rather than a classical batch process (see the Experimental section for details). We have shown in recent work that continuous flow self-assembly of BCPs yields assemblies that are more stable and more reproducible in comparison to aggregates obtained *via* classical methods.[87] Fig. 5 shows some exemplary cryo-TEM images of such a nanoassembly of **5**, which have a typical diameter in the range 30–70 nm. Based on the difference in polarity between the blocks, we expect the aqueous environment to drive the formation of a shell of the polar PMA around the apolar PFO. This core–shell architecture seems to be supported by the fact that the TEM images reveal a defined, relatively dark core surrounded by a lighter colored outer region. The difference in gray scale may well stem from a difference in mass density between the PFO and PMA blocks. This formation of nanoaggregates in solution is a further good indication for the success of the block copolymer synthesis procedure.

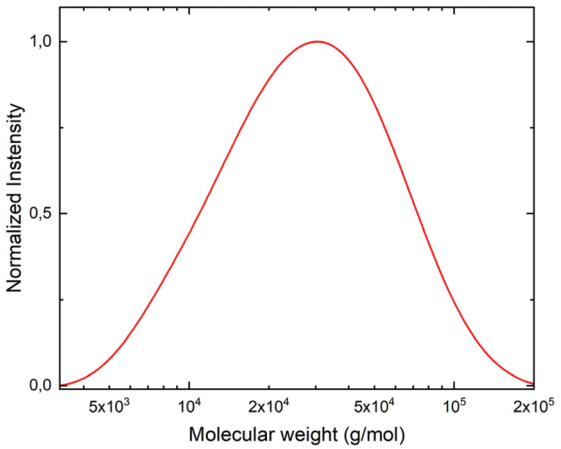

Fig. 4 Molecular weight distribution of PMA-*b*-PFO-*b*-PMA tri-BCP **5**, measured by GPC against polystyrene standards and using THF as the mobile phase.

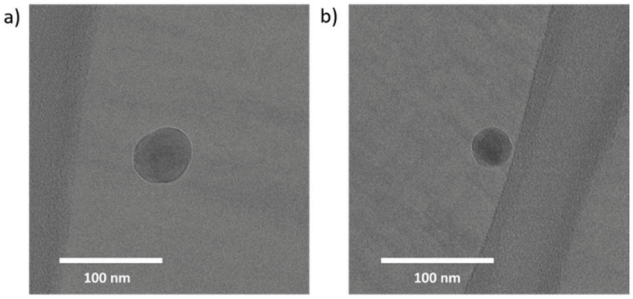

Fig. 5 Cryo-TEM images of nanoaggregates of PMA-*b*-PFO-*b*-PMA. Panels a) and b) show two different aggregates.

To examine the effect of the aggregation state of the tri-BCP **5** on its photophysical properties, we recorded its UV-VIS absorption and photoluminescence (PL) spectra in toluene and water (see Fig. 6 and 7a). Fig. 6a and b show the normalized absorption spectra of the polar tri-BCP **5** (in toluene and water), together with those of the apolar tri-BCP **4** and distyryl-PFO precursor **2** as a reference (both in toluene). Besides, to confirm that the RAFT end groups do not quench the PL of the

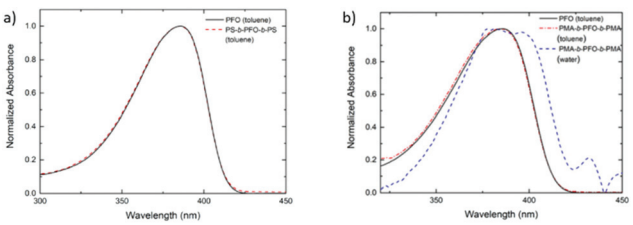

Fig. 6 Normalized UV-Vis absorption spectrum of (a) PS-*b*-PFO-*b*-PS **4** in toluene and (b) PMA-*b*-PFO-*b*-PMA **5** in toluene and water. The absorption spectrum of distyryl-PFO (**2**) in toluene is added to each panel as a reference.

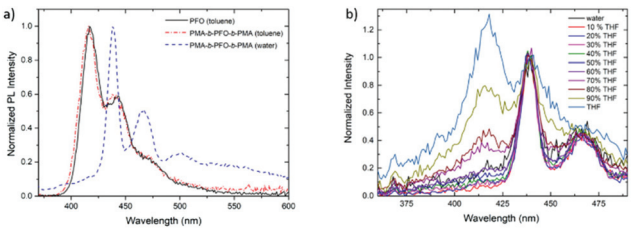

Fig. 7 (a) Normalized steady state photoluminescence (PL) spectra of PMA-*b*-PFO-*b*-PMA **5** in toluene and water. The PL spectrum of distyryl-PFO (**2**) in toluene is added as a reference. (b) Normalized PL spectrum of **5** in water : THF mixtures plotted as a function of THF content (see legend).

PFO block, we performed comparative PL quantum yield (PLQY) measurements on **2** and **4** and indeed observed no difference (see ESI, section S2†). Fig. 6 shows that in an apolar solvent the spectra of the blockcopolymers are highly similar to that of the distyryl-PFO homopolymer. The featureless band with a maximum at ~380 nm is consistent with absorption by PFO chains with a high conformational disorder.[88–91] Strikingly, significant spectral changes are observed upon dispersing the amphiphilic PMA-*b*-PFO-*b*-PMA tri-BCP **5** in water (dashed blue spectrum in Fig. 6b). The spectrum becomes more structured, red-shifts and exhibits a "new" feature at λ = 436 nm. All these changes are consistent with the formation of a significant fraction of β-phase PFO upon self-assembly of tri-BCP **5**.[89,91,92]

The formation of β-phase PFO in the nanoaggregates of **5** is also expressed by their light-emitting properties, which we studied by performing photoluminescence (PL) measurements of the aqueous dispersion. Fig. 7a plots the emission spectrum (dashed blue line) together with that of **5** in toluene (dashed red line) and that of distyryl-PFO **2** (black line) as a reference. As also seen in case of the absorption spectra, in toluene the emission spectrum of tri-BCP **5** is highly similar to that of **2** and consistent with emission from disordered PFO. However, upon dispersion of **5** in water, the fine structure becomes more pronounced upon the rearrangement of the dioctylfluorene monomers in the ordered and rather planarized all-gauge conformation, characteristic to the β-phase.

The resulting increase in conjugation length suppresses the HOMO–LUMO gap and causes a red-shift of the dominant transitions to, respectively, 438, 466 and 500 nm. The fact that the emission spectrum of the self-assembled aggregates is fully dominated by β-phase PFO, where it only represents a minor contribution to the absorption spectrum, is not surprising. Energy transfer from the amorphous (disordered) phase to the β-phase is known to be very efficient.[93] For this reason, only a few volume percent of β-phase suffices to fully dominate the emission spectrum.[94,95] We can interpolate between the emission spectra of the disordered phase and the β-phase by titrating THF into the aqueous dispersion, which controls the aggregation state between fully assembled and molecularly dissolved. Fig. 7b shows the normalized PL spectrum of **5** as a function of THF content. For a THF content between ~40% and 100%, the spectrum is a superposition of β-phase emission and the more blue-shifted amorphous contribution. At 100% THF the BCP is (almost) completely dissolved, evidenced by the fact that the spectrum is fully dominated by the disordered phase (compare: Fig. 7a, red line). This experiment shows that owing to the combination of its amphiphilicity and the phase transition in the PFO, the PMA-*b*-PFO-*b*-PMA tri-BCP is capable of sensing the polarity of its aqueous environment.

Conclusions

In this study we introduce a straightforward and clean method to synthesize conjugated triblockcopolymers (tri-BCPs) using RAFT polymerization. The strategy circumvents known disadvantages associated with transition metal- or nitroxide-mediated polymerizations. The method involves the addition of a RAFT agent to a distyryl-endcapped conjugated polymer, in this case poly(dioctylfluorene) (PFO), prior synthesized by a Yamamoto polycondensation. Controlled growth of nonconjugated blocks is accomplished by subsequent use of the resulting PFO-macroinitiator in a RAFT polymerization. The versatility of the method is confirmed by the use of both nonpolar (styrene) and polar (methyl acrylate) monomers in the reaction. As shown by NMR and GPC, the molecular weight of the obtained PS-*b*-PFO-*b*-PS and PMA-*b*-PFO-*b*-PMA tri-BCPs can be well-controlled and exhibits a low dispersity. Although the emphasis of this work is on presenting this novel synthetic approach, we investigate the self-assembly of both tri-BCPs. AFM analysis of thermally annealed films of the nonpolar PS-*b*-PFO-*b*-PS reveals domains containing nanostructures with a lateral periodicity commensurate with classical BCP phase separated morphologies. The amphiphilic PMA-*b*-PFO-*b*-PMA micellizes in aqueous solution, seemingly into core–shell nanoparticles with a diameter around 50 nm. Upon micellization, the PFO blocks partly organizes into the β-phase, evidenced by characteristic features appearing in the absorption spectrum of the aqueous dispersion of PMA-*b*-PFO-*b*-PMA. A clear red-shift of the luminescence spectrum confirms complete energy transfer from the amorphous to the β-phase fraction. Titration of THF into the aqueous dispersion recovers the spectrum of amorphous PFO due to dissolution of the micelles. In short, a simple, clean and general method is introduced to synthesize nonconjugated-conjugated-nonconjugated triblockcopolymers exhibiting tunable properties, relevant to diverse optoelectronic applications, both in solution and the solid state.

Experimental

Materials

The monomers styrene (Merck, ≥99%) and methyl acrylate (MA, Merck ≥99%) were deinhibited over a column of activated basic alumina prior to use. 2-2′-Azoisobutyronitrile (AIBN, Sigma-Aldrich, 12 wt% in acetone) was recrystallized twice from methanol prior to use. The RAFT agent 2-cyano-2-propyl ethyl trithiocarbonate (CPE-TTC) was synthesized according to literature procedures.[96] Bis(1,5-cyclooctadiene)nickel(0) (Sigma-Aldrich), 2,2′-bipyridine (Fisher Chemical, ≥99,5%), 1,5-cyclooctadiene (Sigma-Aldrich, ≥99%), 4-bromostyrene (Alfa Aesar, ≥98%) hydrochloric acid (Merck Chemicals, fuming ≥37%), ethylenediaminetetraacetic acid disodium salt dehydrate (EDTA, Merck Chemicals, ≥99%), sodium bicarbonate (Acros Organics, ≥99.5%), toluene (Merck, ≥99%), methanol (Scharlau chemicals, 99.9%), *N*,*N*-dimethylformamide (Merck, ≥99%), acetone (Chem-Supply, 99.8%), chloroform (Fisher Chemical, ≥99.8%), and chloroform-d (Cambridge isotope Laboratories, 99.8%) or (Sigma-Aldrich, ≥99%), were used without further purification.

Methods

Size-exclusion chromatography (SEC). Analysis of the molecular weight (distributions) of the polymer samples was performed on a PSS SECcurity^2 GPC system operated by PSS WinGPC software, equipped with a SDV 5.0 μm guard column (50 × 8 mm), followed by three SDV analytical 5.0 μm columns with varying porosity (1000 Å, 100 000 Å and 1 000 000 Å) (50 × 8 mm) and a differential refractive index detector using tetrahydrofuran (THF, RCI Labscan, 99.9%) as the eluent at 40 °C with a flow rate of 1 mL min^{-1}. The SEC system was calibrated using linear narrow polystyrene standards ranging from 682 to 2.52×10^6 g mol^{-1} PS ($K = 14.1 \times 10^{-5}$ dL g^{-1} and $\alpha = 0.70$).

Nuclear magnetic resonance (NMR) spectroscopy. 1D proton (^{1}H) NMR were recorded in deuterated chloroform on a Bruker DRX600 NMR spectrometer (14.1 Tesla magnet). NMR spectra were collected and analyzed in MestReNova and Bruker's TopSpin™ software packages. 2D diffusion-ordered NMR spectroscopy (DOSY NMR) measurements were recorded in deuterated chloroform on a Bruker DRX 700 MHz Spectrometer equipped with a commercial Bruker 5 mm 2 channel inversed probe head with *z*-gradients. The dstebpgp3s[1] (2D Double-Stimulated Echo Experiment (DSTE) using bipolar gradients) pulse program was used with the following acquisition parameters: F2 and F1 spectral widths, 13.99 ppm/2.86 ppm. F2 and F1 resolution 0.6 Hz per pt and 125.1 Hz per pt. 32 FIDs were recorded each consisting of 32 scans and 32 768 data points (AQ = 1.67 s). The relaxation delay was 3s. The diffusion time was 0.1s and the gradient pulses Gz(1) and Gz(2) were 1.5 ms and 0.6 ms. DOSY NMR spectra were collected and analyzed in MestReNova and Bruker's TopSpin™ software packages.

Luminescence spectroscopy. To record photoluminescence quantum yields and photolumi-nescence (PL) spectra, we used a HORIBA Jobin Yvon Fluorolog-3 spectrofluorometer, using FluorEssence software. The solutions studied in the spectrofluorimeter were diluted to maintain the absorbance maximum <0.1.

Atomic force microscopy (AFM). AFM images were taken with a Bruker–Dimension Icon FS with ScanAsyst using an OPUS 160AC-NA Cantilever Type at frequency = 300 kHz in tapping mode.

UV-Vis spectroscopy. The absorption measurements were recorded using a PerkinElmer Lambda 900 UV-VIS-NIR Spectrometer.

Film annealing procedure

The films were prepared by spin-coating distyrene end-capped PFO (0.9 wt%) or PS-*b*-PFO-*b*-PS triblockcopolymer (1.4 wt%) from a chloroform solution onto a glass substrate. The films were placed under a nitrogen atmosphere, heated at 250 °C for 2h and subsequently conditioned at 130 °C for 17 h.

Titration of PMA-*b*-PFO-*b*-PMA triblockcopolymer with water/THF

The photoluminescence spectra of PS-*b*-PFO-*b*-PS triblockcopolymer were recorded from different samples containing different ratios of water and THF. The values were changed in a ratio of 10% each between 100% THF and 100% water.

Synthetic procedures

Synthesis and end functionalizing of distyrene end-capped PFO. The polymerization was performed by a Yamamoto coupling reaction. To a mixture of 4 g (14.5 mmol, 2.3 eq.) bis(1,5-cyclooctadiene)nickel(0) and 2.26 g (14.5 mmol, 2.3 eq.) of 2,2′-bipyridine in 35 mL of DMF and 200 mL of toluene, a solution of 3.46 g of 1,1′-dioctyl-2,7-dibromofluorene (6.3 mmol, 1.0 eq.) in 10 mL of toluene was added. Solutions and flasks were degassed in advance. The mixture was heated to 80 °C and kept stirring for 4 minutes under a nitrogen atmosphere. For end group functionalization, 0.98 mL (8.0 mmol, 1.3 eq.) 1,5-cyclooctadiene and 4.6 g (25.1 mmol, 4.0 eq.) 4-bromostyrene were added. The resulting solution was stirred for 6 minutes and kept under a nitrogen atmosphere. The reaction was terminated by adding 10 mL of 4 M HCl and the solution was kept stirring for 15 minutes. After cooling down to room temperature, the mixture was transferred to a separation funnel and 200 mL of 2 M HCL was added. After vigorous mixing, the phases were separated, and the organic phase was washed with 200 mL of 2 M HCl. The organic phase was washed with 200 mL of ethylenediaminetetraacetic acid disodium salt dihydrate (EDTA-Na_2) solution, 200 mL of sodium bicarbonate solution and again 200 mL of EDTA-Na_2 solution. The resulting organic phase was filtered through silica gel, concentrated by using a rotatory evaporator and the polymer was precipitated in excess methanol. Impurities and low molecular weight chains were then removed by a Soxhlet apparatus with acetone for 5 days. The obtained polymer was then dried overnight under vacuum and samples for ^{1}H NMR and GPC were collected. GPC (THF): M_n = 15 360 g mol^{-1}, M_w = 29 200 g mol^{-1} and $Đ$ = 1.90; ^{1}H NMR (600 MHz, $CDCl_3$) δ in ppm: 7.84 (m, 2H, Ar–H), 7.68 (m, 4H, Ar–H), 7.60 (m, 4H, CH), 7.53 (m, 4H, CH), 6.80 (dd, 2H, CH), 5.84 (dd, 2H, CH_2), 5.31 (dd, 2H, CH_2), 2.13 (m, 4H, CH_2), 1.15 (m, 24H, CH_2), 0.83 (m, 10H, CH_2/CH_3).

Synthesis of PFO-macro-RAFT agent (di-CPETTC-PFO). 200 mg (0.012 mmol, 1 eq.) of PFO (approx. 17 000 g mol^{-1}) was added to a flask equipped with a stirring bar and dissolved in 20 mL toluene by heating up to 50 °C. Subsequently, 2 mg (0.012 mmol, 1 eq.) of AIBN and 50 mg (0.24 mmol, 20.3 eq.) of the RAFT agent 2-cyano-2-propyl ethyl trithiocarbonate (CPE-TTC) was added to the solution. The mixture was degassed by purging with nitrogen for 20 minutes. The solution was then heated up to 70 °C and kept stirring overnight under a nitrogen atmosphere and an aliquot was collected for^{1}H NMR analysis. Next, 2.5 mg (0.015 mmol, 1.2 eq.) of AIBN and 1 ml toluene were added to the mixture. The solution was purged with nitrogen for 5 minutes, heated up to 70 °C and kept stirring overnight under a nitrogen atmosphere. Afterwards, a sample for ^{1}H NMR was collected. In order to increase the yield, 3.3 mg (0.02 mmol, 1.7 eq.) of AIBN and 42 mg (0.20 mmol, 16.7 eq.) of the RAFT agent (CPE-TTC) were added to the mixture. After

purging with nitrogen for 10 minutes, the mixture was heated up to 70 °C and kept stirring overnight under a nitrogen atmosphere. The endgroup functionalized polymer obtained was then precipitated twice in excess methanol, centrifuged and dried overnight under vacuum to obtain 110mg of a yellowish powder. Samples were then collected for ^{1}H NMR and GPC analysis. GPC in THF: M_n = 19 500 g mol^{-1}, M_w = 29 450 g mol^{-1} and $Đ$ = 1.51; ^{1}H NMR (600 MHz, $CDCl_3$) δ in ppm: 7.84 (m, 2H, Ar–H), 7.68 (m, 4H, Ar–H), 7.59 (m, 4H, CH), 7.51 (m, 4H, CH), 5.53 (m, 2H, CH), 3.37 (m, 4H, CH_2), 2.13 (m, 4H, CH_2), 1.58 (m, 18H, CH_3), 1.15 (m, 24H, CH_2), 0.82 (m, 10H, CH_2/CH_3).

Synthesis of the PS-*b*-PFO-*b*-PS triblockcopolymer. 20 mg (0.001mmol, 1 eq.) of di-CPETTC-PFO (approx. 17 000 g mol^{-1}) initiator was dissolved in 2.3 mL toluene by heating up to 50 °C. 0.20 mg VAZO88 (0.0008 mmol, 0.7 eq.) and 1.14 mL styrene (10 mmol, 9090 eq.) were added to the solution. The solution was purged with nitrogen for 20 minutes. Subsequently the solution was heated up to 90 °C and kept stirring for 180 minutes under a nitrogen atmosphere. The polymer was then precipitated in excess methanol and dried overnight under vacuum. 126 mg of a yellowish powder was obtained. Samples were collected for ^{1}H NMR, GPC, UV-VIS and photoluminescence analysis. GPC in THF: M_n = 50 000 g mol^{-1}, M_w = 86 000 g mol^{-1} and $Đ$ = 1.72; ^{1}H NMR (600 MHz, $CDCl_3$) δ in ppm: 7.85 (m, 2H, Ar–H_{PFO}), 7.69 (m, 4H, Ar–H_{PFO}), 7.60 (m, 4H, CH), 7.52 (m, 4H, CH), 7.04 (m, 6H, Ar–H_{PS}), 6.58 (m, 4H, Ar–H_{PS}), 2.13 (m, 4H, $CH_{2,\ PFO}$), 1.87 (m, 2H, CH_{PS}), 1.44 (m, 4H, $CH_{2,\ PS}$), 1.15 (m, 24H, $CH_{2,\ PFO}$), 0.82 (m, 10H, CH_2/$CH_{3,\ PFO}$).

Synthesis of the PMA-*b*-PFO-*b*-PMA triblockcopolymer. 40 mg (0.002 mmol, 1 eq.) of PFO-RAFT (approx. 17 000 g mol^{-1}) initiator was dissolved in 2.3 mL toluene by heating up to 50 °C. 0.04 mg AIBN (0.0016 mmol, 0.1 eq.) and 2.05 mg of methyl acrylate (0.024 mmol, 10 eq.) were added to the solution. Oxygen was removed from the mixture by a freeze pump thaw cycle repeated 5 times. Subsequently the solution was heated up to 70 °C and kept stirring overnight under an argon atmosphere. The polymer was then precipitated in excess methanol and dried under vacuum. A yellowish powder was obtained. A sample was collected for GPC analysis. GPC in THF: M_n = 21 120 g mol^{-1}, M_w = 35 440 g mol^{-1} and $Đ$ = 1.67.

Conflicts of interest

There are no conflicts to declare.

Acknowledgements

The authors acknowledge the Deutscher Akademischer Austauschdienst (DAAD) and Universities Australia (UA) for financial support through Project 57446038. Open Access funding provided by the Max Planck Society.

References

1 X. Feng, F. LV, L. Liu, H. Tang, C. Ching, Q. Yang and S. Wang, *ACS Appl. Mater. Interfaces*, 2010, **2**, 2429–2435.
2 X. L. Chen and S. A. Jenekhe, *Macromolecules*, 1996, **29**, 6189–6192.
3 F. Meyers, A. Heeger and J. Brédas, *J. Chem. Phys.*, 1992, **97**, 2750–2758.
4 I. Botiz and S. B. Darling, *Mater. Today*, 2010, **13**, 42–51.
5 J. Zhang, K. Kremer, J. J. Michels and K. C. Daoulas, *Macromolecules*, 2020, **53**, 523–538.
6 G. Ren, P.-T. Wu and S. A. Jenekhe, *ACS Nano*, 2011, **5**, 376–384.
7 S. Lu, T. Liu, L. Ke, D.-G. Ma, S.-J. Chua and W. Huang, *Macromolecules*, 2005, **38**, 8494–8502.
8 I. Cosemans, J. Vandenbergh, L. Lutsen, D. Vanderzande and T. Junkers, *Polym. Chem.*, 2013, **4**, 3471–3479.
9 N. Zaquen, H. Lu, T. Chang, R. Mamdooh, L. Lutsen, D. Vanderzande, M. Stenzel and T. Junkers, *Biomacromolecules*, 2016, **17**, 4086–4094.
10 Y. Zhao, F. Sakai, L. Su, Y. Liu, K. Wei, G. Chen and M. Jiang, *Adv. Mater.*, 2013, **25**, 5215–5256.
11 Y.-C. Chiang, S. Kobayashi, T. Isono, C.-C. Shih, T. Shingu, C.-C. Hung, H.-C. Hsieh, S.-H. Tung, T. Satoh and W.-C. Chen, *Polym. Chem.*, 2019, **10**, 5452–5464.
12 S. Mahajan, *Encyclopedia of materials: science and technology*, Elsevier, Oxford, 2001.
13 N. Hadjichristidis, S. Pispas and G. Floudas, *Block copolymers: synthetic strategies, physical properties, and applications*, John Wiley & Sons, New Jersey, 2003.
14 M. Lazzari, G. Liu and S. Lecommandoux, *Block copolymers in nanoscience*, John Wiley & Sons, Weinheim, 2006.
15 Y.-C. Tseng and S. B. Darling, *Polymers*, 2010, **2**, 470–489.
16 C.-H. Lin, Y. C. Tung, J. Ruokolainen, R. Mezzenga and W.-C. Chen, *Macromolecules*, 2008, **41**, 8759–8769.
17 B. McCulloch, G. Portale, W. Bras, J. A. Pople, A. Hexemer and R. A. Segalman, *Macromolecules*, 2013, **46**, 4462–4471.
18 B. D. Olsen, M. Shah, V. Ganesan and R. A. Segalman, *Macromolecules*, 2008, **41**, 6809–6817.
19 J. Chen, E. L. Thomas, C. K. Ober and G.-P. Mao, *Science*, 1996, **273**, 343–346.
20 C.-L. Liu, C.-H. Lin, C.-C. Kuo, S.-T. Lin and W.-C. Chen, *Prog. Polym. Sci.*, 2011, **36**, 603–637.
21 D. Marsitzky, M. Klapper and K. Müllen, *Macromolecules*, 1999, **32**, 8685–8688.
22 N. Zaquen, K. Verstraete, L. Lutsen, D. Vanderzande and T. Junkers, *Polym. Chem.*, 2016, **7**, 4771–4781.
23 I. Cosemans, J. Vandenbergh, L. Lutsen, D. Vanderzande and T. Junkers, *Polym. Chem.*, 2013, **4**, 3471–3479.
24 M. Surin, D. Marsitzky, A. C. Grimsdale, K. Müllen, R. Lazzaroni and P. Leclèreet, *Adv. Funct. Mater.*, 2004, **14**, 708–715.
25 V. Francke, H. J. Räder, Y. Geerts and K. Müllen, *Macromol. Rapid Commun.*, 1998, **19**, 275–281.
26 H. Wang, W. You, P. Jiang, L. Yu and H. H. Wang, *Chem. – Eur. J.*, 2004, **10**, 986–993.

27 N. Sary, R. Mezzenga, C. Brochon, G. Hadziioannou and J. Ruokolainen, *Macromolecules*, 2007, **40**, 3277–3286.
28 N. Sary, L. Rubatat, C. Brochon, G. Hadziioannou, J. Ruokolainen and R. Mezzenga, *Macromolecules*, 2007, **40**, 6990–6997.
29 B. D. Olsen and R. A. Segalman, *Macromolecules*, 2005, **38**, 10127–10137.
30 C.-C. Ho, Y.-H. Lee, C.-A. Dai, R. A. Segalman and W.-F. Su, *Macromolecules*, 2009, **42**, 4208–4219.
31 G. Tu, H. Li, M. Forster, R. Heiderhoff, L. J. Balk and U. Scherf, *Macromolecules*, 2006, **39**, 4327–4331.
32 K. A. Smith, Y.-H. Lin, D. B. Dement, J. Strzalka, S. B. Darling, D. L. Pickel and R. Verduzco, *Macromolecules*, 2013, **46**, 2636–2645.
33 A. N. Le, R. Liang and M. Zhong, *Chem. – Eur. J.*, 2019, **25**, 8177–8189.
34 U. Stalmach, B. de Boer, C. Videlot, P. F. van Hutten and G. Hadziioannou, *J. Am. Chem. Soc.*, 2000, **122**, 5464–5472.
35 S. Lu, Q.-L. Fan, S.-Y. Liu, S.-J. Chua and W. Huang, *Macromolecules*, 2002, **35**, 9875–9881.
36 P. K. Tsolakis and J. K. Kallitsis, *Chem. – Eur. J.*, 2003, **9**, 936–943.
37 W. Wang, R. Wang, C. Zhang, S. Lu and T. Liu, *Polymer*, 2009, **50**, 1236–1245.
38 S. Lu, Q.-L. Fan, S.-J. Chua and W. Huang, *Macromolecules*, 2003, **36**, 304–310.
39 Y. Tian, C.-Y. Chen, H.-L. Yip, W.-C. Wu, W.-C. Chen and A. K.-Y. Jen, *Macromolecules*, 2010, **43**, 282–291.
40 N. Zaquen, J. Vandenbergh, M. Schneider-Baumann, L. Lutsen, D. Vanderzande and T. Junkers, *Polymers*, 2015, **7**, 418–452.
41 U. Stalmach, B. de Boer, A. D. Post, P. F. van Hutten and G. Hadziioannou, *Angew. Chem., Int. Ed.*, 2001, **40**, 428–430.
42 B. de Boer, U. Stalmach, H. Nijland and G. Hadziioannou, *Adv. Mater.*, 2000, **12**, 1581–1583.
43 B. de Boer, U. Stalmach, P. F. van Hutten, C. Melzer, V. V. Krasnikov and G. Hadziioannou, *Polymer*, 2001, **42**, 9097–9109.
44 B. François, G. Widawski, M. Rawiso and B. Cesar, *Synth. Methods*, 1995, **69**, 463–466.
45 X. F. Zhong and B. François, *Makromol. Chem.*, 1991, **192**, 2277–2291.
46 G. C. Bazan, Y.-J. Miao, M. L. Renak and B. J. Sun, *J. Am. Chem. Soc.*, 1996, **118**, 2618–2624.
47 C. P. Radano, O. A. Scherman, N. Stingelin-Stutzmann, C. Müller, D. W. Breiby, P. Smith, R. A. J. Janssen and E. W. Meijer, *J. Am. Chem. Soc.*, 2005, **127**, 12502–12503.
48 A. de Cuendias, M. Le Hellaye, S. Lecommandoux, E. Cloutet and H. Cramail, *J. Mater. Chem.*, 2005, **15**, 3264–3267.
49 U. Scherf, A. Gutacker and N. Koenen, *Acc. Chem. Res.*, 2008, **41**, 1086–1097.
50 U. Asawapirom, R. Güntner, M. Forster, U. Scherf, *et al.*, *Thin Solid Films*, 2005, **477**, 48–52.
51 X. Xiao, Y. Fu, M. Sun, L. Li and Z. Bo, *J. Polym. Sci., Part A: Polym. Chem.*, 2007, **45**, 2410–2424.
52 G. Tu, H. Li, M. Forster, R. Heiderhoff, L. J. Balk, R. Sigel and U. Scherf, *Small*, 2007, **3**, 1001–1006.
53 T. Yokozawa, R. Suzuki, M. Nojima, Y. Ohta and A. Yokoyama, *Macromol. Rapid Commun.*, 2011, **32**, 801–806.
54 C. Brochon, N. Sary, R. Mezzenga, C. Ngov, F. Richard, M. May and G. Hadziioannouet, *J. Appl. Polym. Sci.*, 2008, **110**, 3664–3670.
55 H. De Brouwer, M. A. J. Schellekens, B. Klumperman, M. J. Monteiro and A. L. German, *J. Polym. Sci., Part A: Polym. Chem.*, 2000, **38**, 3596–3603.
56 G. Moad, E. Rizzardo and S. H. Thang, *Aust. J. Chem.*, 2005, **58**, 379–410.
57 M. Arcana, K. Nagesh and R. Rama, *J. Eng. Technol. Sci.*, 2004, **36**, 63–79.
58 G. Moad, M. Chen, M. Häussler, A. Postma, E. Rizzardo and S. H. Thang, *Polym. Chem.*, 2011, **2**, 492–519.
59 S. Perrier, *Macromolecules*, 2017, **50**, 7433–7447.
60 X. Xiao, Y.-q. Fu, J.-j. Zhou, Z.-s. Bo, L. Li, C.-M. Chan, *et al.*, *Macromol. Rapid Commun.*, 2007, **28**, 1003–1009.
61 M. Chen, M. Häussler, G. Moad and E. Rizzardo, *Org. Biomol. Chem.*, 2011, **9**, 6111–6119.
62 Q. Zhang, L. Chi, G. Hai, Y. Fang, X. Li, R. Xia, W. Huang and E. Gu, *Molecules*, 2017, **22**, 315.
63 M. Ariu, D. Lidzey and D. Bradley, *Synth. Met.*, 2000, **111**, 607–610.
64 M. Ariu, M. Sims, M. D. Rahn, J. Hill, A. M. Fox, D. G. Lidzey, M. Oda, J. Cabanillas-Gonzalez and D. D. C. Bradley, *Phys. Rev. B: Condens. Matter Mater. Phys.*, 2003, **67**, 195333.
65 A. Perevedentsev, N. Chander, J.-S. Kim and D. D. C. Bradley, *J. Polym. Sci., Part B: Polym. Phys.*, 2016, **54**, 1995–2006.
66 T. Yamamoto, Y. Hayashi and A. Yamamoto, *Chem. Soc. Jpn.*, 1978, **51**, 2091–2097.
67 H. Yeo, K. Tanaka and Y. Chujo, *J. Polym. Sci., Part A: Polym. Chem.*, 2012, **50**, 4433–4442.
68 W.-J. Li, B. Liu, Y. Qian, L.-H. Xie, J. Wang, S.-B. Li and W. Huang, *Polym. Chem.*, 2013, **4**, 1796–1802.
69 J. Langecker and M. Rehahn, *Macromol. Chem. Phys.*, 2008, **209**, 258–271.
70 Y. Bakkour, V. Darcos, S. Li and J. Coudane, *Polym. Chem.*, 2012, **3**, 2006–2010.
71 W. Li, H. Chung, C. Daeffler, J. A. Johnson and R. H. Grubbs, *Macromolecules*, 2012, **45**, 9595–9603.
72 J. Martin, E. C. Davidson, C. Greco, W. Xu, J. H. Bannock, A. Agirre, J. de Mello, R. A. Segalman, N. Stingelin and K. C. Daoulas, *Chem. Mater.*, 2018, **30**, 748–761.
73 J. R. Sargent and W. P. Weber, *J. Polym. Sci., Part A: Polym. Chem.*, 2000, **38**, 482–488.
74 U. Tunca, T. Erdogan and G. Hizal, *J. Polym. Sci., Part A: Polym. Chem.*, 2002, **40**, 2025–2032.
75 S. Schöttner, R. Hossain, C. Rüttiger, M. Gallei, *et al.*, *Polymers*, 2017, **9**, 491.
76 Z. Xu, T. Liu, K. Cao, D. Guo, J. M. Serrano and G. Liu, *ACS Appl. Polym. Mater.*, 2020, **2**, 1398–1405.

77 L. Charles, *Mass Spectrom. Rev.*, 2014, **33**, 523–543.
78 M. Grell, D. D. C. Bradley, G. Ungar, J. Hill and K. S. Whitehead, *Macromolecules*, 1999, **32**, 5810–5817.
79 G. Ryu, P. N. Stavrinou and D. D. Bradley, *Adv. Funct. Mater.*, 2009, **19**, 3237–3242.
80 M. Campoy-Quiles, M. Sims, P. G. Etchegoin and D. D. C. Bradley, *Macromolecules*, 2006, **39**, 7673–7680.
81 J. Rieger, *J. Therm. Anal. Calorim.*, 1996, **46**, 965–972.
82 E. Thomas and R. Lescanec, Phase morphology in block copolymer systems, *Philos. Trans. R. Soc., A*, 1994, **348**, 149–166.
83 R. Verduzco, I. Botiz, D. L. Pickel, S. M. Kilbey, K. Hong, E. Dimasi and S. B. Darlinget, *Macromolecules*, 2011, **44**, 530–539.
84 M. Appold, J. Bareuther and M. Gallei, *Macromol. Chem. Phys.*, 2019, **220**, 1800548.
85 Y. Lu, E. Zhang, J. Yang and Z. Cao, *Nano Res.*, 2018, **11**, 4985–4998.
86 Y. Mai and A. Eisenberg, *Chem. Soc. Rev.*, 2012, **41**, 5969–5985.
87 A. L. Buckinx, K. Verstraete, E. Baeten, R. F. Tabor, A. Sokolova, N. Zaquen and T. Junkers, *Angew. Chem.*, 2019, **58**, 13799–13802.
88 U. Scherf and E. J. List, *Adv. Mater.*, 2002, **14**, 477–487.
89 A. J. Cadby, P. A. Lane, H. Mellor, S. J. Martin, M. Grell, C. Giebeler, D. D. C. Bradley, M. Wohlgenannt, C. An and Z. V. Vardeny, *Phys. Rev. B: Condens. Matter Mater. Phys.*, 2000, **62**, 15604.
90 F. B. Dias, J. Morgado, A. L. Maçanita, F. P. da Costa, H. D. Burrows and A. P. Monkman, *Macromolecules*, 2006, **39**, 5854–5864.
91 U. Scherf and D. Neher, *Polyfluorenes*, Springer, Heidelberg, 2008.
92 M.-N. Yu, H. Soleimaninejad, J.-Y. Lin, Z.-Y. Zuo, B. Liu, Y.-F. Bo, L.-B. Bai, Y.-M. Han, T. A. Smith, M. Xu, X.-P. Wu, D. E. Dunstan, R.-D. Xia, L.-H. Xie, D. D. C. Bradley, W. Huang and J. Phys, *Chem. Lett.*, 2018, **9**, 364–372.
93 M. Ariu, D. G. Lidzey, M. Sims, A. J. Cadby, P. A. Lane and D. D. C. Bradley, *J. Phys.: Condens. Matter*, 2002, **14**, 9975.
94 E. Khodabakhshi, P. W. Blom and J. J. Michels, *Appl. Phys. Lett.*, 2019, **114**, 093301.
95 H.-H. Lu, C.-Y. Liu, C.-H. Chang and S.-A. Chen, *Adv. Mater.*, 2007, **19**, 2574–2579.
96 Y. K. Chong, G. Moad, E. Rizzardo and S. H. Thang, *Macromolecules*, 2007, **40**, 4446–4455.